

A Modeling Framework for Bioretention Analysis: Assessing the Hydrological Performance under System's Uncertainty (Supplemental Material)

Marcus Nóbrega Gomes Júnior^{1*}, Marcio H. Giacomoni², Marina B. de Macedo³, César A. F. do Lago⁴, José A. T. Brasil⁵, Thalita R. P. de Oliveira⁶, Eduardo M. Mendiando⁷

I. MATHEMATICAL FORMULATION

The bioretention dynamical model described in this paper assumes as dynamical state variables a vector containing a part of dynamical variables and the remainder of algebraic variables, such that $\mathbf{x}_1(t) = [L(t), h(t), S(t)]^T$ and $\mathbf{x}_2(t) = [Q_{\text{out}}(t), Q_{\text{out,u}}(t), Q_{\text{out,w}}(t), Q_{\text{exf}}(t), Q_{\text{inf}}(t)]^T$. The concatenated state-vector is defined as $\mathbf{x}(t) = [\mathbf{x}_1(t), \mathbf{x}_2(t)]^T$. The non-linear bioretention dynamical model can be written in a non-linear differential-algebraic model, constrained by energy and mass balance equations, such that

$$\mathbf{E}\dot{\mathbf{x}}(t) = \mathbf{A}\mathbf{x}(t) + \mathbf{\Phi}(\mathbf{x}(t)) \quad (\text{S1})$$

where $\mathbf{E} \in \mathbb{R}^{9 \times 9}$ is a singular matrix with some zero rows, $\mathbf{A} \in \mathbb{R}^{9 \times 9}$ is a system matrix and $\mathbf{\Phi}(\mathbf{x}(t)) \in \mathbb{R}^{9 \times 1}$ a non-linear state vector.

¹Ph.D. Candidate, Department of Civil and Environmental Engineering, The University of Texas at San Antonio, One UTSA Circle, BSE 1.310, TX 78249. Ph.D. Candidate, Department of Hydraulic Engineering and Sanitation, University of São Paulo, São Carlos School of Engineering, Av. Trab. São Carlense, 400 - Centro, São Carlos - SP, 13566-590, ORCID: <https://orcid.org/0000-0002-8250-8195>, Email: marcusnobrega.engcivil@gmail.com. * Corresponding author.

²Associate Professor, Department of Civil and Environmental Engineering, The University of Texas at San Antonio, One UTSA Circle, BSE 1.346, TX 78249, ORCID: <https://orcid.org/0000-0001-7027-4128>, Email: marcio.giacomoni@utsa.edu.

³Assistant Professor, Institute of Natural Resources, Federal University of Itajubá, Itajubá, Minas Gerais, Brazil, 37500-903, ORCID: <https://orcid.org/0000-0003-2829-754X>, Email: marinamacedo@unifei.edu.br

⁴Ph.D. Candidate, Department of Civil and Environmental Engineering, The University of Texas at San Antonio, One UTSA Circle, BSE 1.310, TX 78249. ORCID: <https://orcid.org/0000-0002-8250-8195>, Email: cesar.dolago@utsa.edu

⁵Ph.D. Student, Department of Civil and Environmental Engineering, The University of Texas at San Antonio, One UTSA Circle, BSE 1.310, TX 78249. ORCID: <https://orcid.org/0000-0002-0331-0122>, Email: Jose.Brasil@utsa.edu

⁶M.Sc., Department of Hydraulic Engineering and Sanitation, University of São Paulo, São Carlos School of Engineering, Av. Trab. São Carlense, 400 - Centro, São Carlos - SP, 13566-590, ORCID: <https://orcid.org/0000-0002-7841-046X>, Email: thalitarauel96@gmail.com

⁷Associate Professor, Department of Hydraulic Engineering and Sanitation, University of São Paulo, São Carlos School of Engineering, Av. Trab. São Carlense, 400 - Centro, São Carlos - SP, 13566-590, ORCID: <https://orcid.org/0000-0003-2319-2773>, Email: emm@sc.usp.br

This work was financially supported by the São Paulo Research Foundation (FAPESP) grants [# 2018/20865-0] and [# 2017/21940-2]. The authors gratefully acknowledge the support given by the University of São Paulo - São Carlos School of Engineering for allowing the implementation and monitoring of the laboratory and field scale bioretention systems. The authors also gratefully acknowledge the support given by the National Institute of Science and Technology for Climate Change, Water Security Subcomponent, FAPESP Grant 2014/50848-9.

TABLE S1: Model variables and parameters and paper acronyms.

| Symbol | Description |
|---------------------------------|--|
| $2s$ | Bioretention perimeter (m) |
| ADD | Antecedent Dry Days |
| A_{imp} | Impervious catchment area (m ²) |
| A_o | Orifice area (m ²) |
| AR | Area Ratio given by $A_{\text{TC}}/A_{\text{imp}}$ |
| A_{TC} | Surface bioretention area (m ²) |
| $C_{d,u}$ | Orifice discharge coefficient |
| g | Gravity acceleration = 9.81 m/s ² |
| $h_p(t)$ | Ponding depth (cm) |
| $i(t)$ | Rainfall intensity (mm/h) |
| IWS | Internal Water Storage (cm) |
| K_{sat} | Media saturated hydraulic conductivity (mm/h) |
| $K_{\text{sat},l}$ | Bottom saturated hydraulic conductivity (mm/h) |
| $K_{\text{sat},b}$ | Lateral saturated hydraulic conductivity (mm/h) |
| $L(t)$ | Saturated front (m) |
| L_d | Bioretention depth (m) |
| n_1 | Number of orifices |
| n_2 | Number of weirs |
| $P(t)$ | Average inflow (m ³ /s) |
| p | Weir elevation (m) |
| ψ | Suction head (cm) |
| $q_{\text{ETR}}(t)$ | Evapotranspiration rate in mm/h |
| $Q_{\text{exf}}(t)$ | Exfiltration flow (m ³ /s) |
| $Q_{\text{in}}(t)$ | Total Inflow (m ³ /s) |
| $Q_{\text{inf}}(t)$ | Infiltration flow (m ³ /s) |
| $Q_{\text{per}}(t)$ | Percolation flow (m ³ /s) |
| $q_{\text{inf}}(t)$ | Infiltration rate (mm/h) (m ³ /s) |
| $q_{\text{in}}(t)$ | Inflow rate (mm/h) |
| $Q_{\text{lim}}(t)$ | Maximum allowable outflow (m ³ /s) |
| $Q_{\text{out}}(t)$ | Total outflow (m ³ /s) |
| $Q_{\text{out,r,d}}$ | Maximum outflow per RP, per t_d (m ³ /s) |
| $Q_{\text{out,u}}(t)$ | Underdrain outflow (m ³ /s) |
| $Q_{\text{out,w}}(t)$ | Weir outflow (m ³ /s) |
| Q_{out}^p | Bioretention outflow peak (m ³ /s) |
| $Q_r(t)$ | Catchment runoff rate (m ³ /s) |
| $S(t)$ | Storage (reservoir and ponding zone) |
| s_f | suction head factor $\in [-1, 0, 1]$ |
| \mathcal{T}_{cr} | Critical rainfall duration set |
| t_d | Rainfall duration set (min) |
| t_d | Rainfall duration (min) |
| θ_i | Initial soil moisture (cm ³ .cm ⁻³) |
| θ_{sat} | Saturated soil moisture (cm ³ .cm ⁻³) |
| V_{in} | Internal volume (m ³) |
| $V_{\text{in},*}(t + \Delta t)$ | Internal volume for hortonian flow condition (m ³) |
| V_{in} | Modeled outflow volume |
| V_o | Observed outflow volume |
| V_r | Inflow runoff volume |
| V_r | Volume-ratio (maximum storage / inflow volume) |

A. Inflow Rate From Runnon and Rainfall

The inflow rate $Q_{in}(t)$ into the bioretention includes the runnon into the system $Q_r(t)$ and the direct net rainfall $i(t) - q_{ETP}(t)$, which considers losses through evapotranspiration and is described as:

$$Q_{in}(t) = Q_r(t) + (i(t) - q_{ETR}(t))A_{TC} \quad (S2)$$

For discrete sub-daily events, typically the evapotranspiration can be neglected [1]–[3]. The runnon can be estimated using rainfall-runoff models or assumed with observation data. The inflow rate into the bioretention media $P(t)$ averages the direct instantaneous inflow rate for two consecutive time-steps, normalizes the flow according to the surface area of the bioretention A_{TC} to obtain an equivalent depth rate, and adds any stored volume at the ponding depth $h(t)$ (cm), as described as:

$$P(t) = \left(\frac{Q_{in}(t) + Q_{in}(t + \Delta t)}{2A_{TC}} + \frac{h(t)}{6,000\Delta t} \right) 3.6 \quad (S3)$$

where: Δt is the time-step of the model (min), and the numbers are correcting factors for the given units.

B. Infiltration Capacity Through Green-Ampt Model

The infiltration capacity of the soil media is modeled using the GA equation, which depends on physical soil parameters: initial moisture (θ_i), saturation moisture (θ_{sat}), hydraulic conductivity (K_{sat}), and suction head (ψ) [4]. All parameters are assumed uniformly constant throughout the layers [5]. Because of potential numerical instabilities, especially at the beginning of events when the soil is often dry [3], the model averages the infiltration capacity at the beginning and at the end of the time step (i.e., in this case assuming that all inflow infiltrated into the media). The infiltration capacity at a time interval t can be written following Eq. (S4) and the infiltration rate $q_{inf}(t)$ is the minimum between the infiltration capacity and the inflow rate, in equivalent depth units.

$$C(t) = \frac{1}{2}K_{sat} \left[2 + \frac{1}{100} (s_f \psi + h(t)) L^*(t) \right] \quad (S4)$$

$$L^*(t) = \left[\min \left(L(t) + \frac{V_{in,*}(t + \Delta t) - V_{in}(t)}{(2\theta_{sat} - \theta_i)A_{TC}}, L_d \right) \right]^{-1} \quad (S5)$$

where $V_{in,*}(t + \Delta t) = 0.5[(Q_{in}(t + \Delta t) + Q_{in}(t))\Delta t]$.

The infiltration capacity is calculated using Eq. (S4) with $s_f = 1$ for $h \leq 0$ otherwise $s_f = 0$. The percolation capacity, however, has different values of s_f , such that $s_f = 1$ if $h > 0$ and $L(t) < L_d$ and $L(1 : t) < L_d$. Moreover, if $h >$

0 and $L(t) = L_d$, $s_f = 0$ because the suction head would occur in the top and bottom interfaces. Finally, if $h = 0$ and $L(t) < L_d$ and $L(1 : t) = L_d$, $s_f = -1$ since the suction head would occur only at the top of the unsaturated zone. With these conditions of s_f and Eq. (S4), one can determine infiltration and percolation soil

C. Bioretention Flow Routing Dynamical Equations

Two water balances are derived to solve the complete water balance in the bioretention system, since the system is composed by a free surface reservoir (i.e., ponding zone with a surface weir) and a porous reservoir (sand and gravel layer with an underdrain at the bottom). Assuming a horizontal ponding zone, the Reynolds Transport Theorem [6] can be simplified in a mass balance and be applied into the interfaces between both reservoirs and at the wetting front. The media water balance, the ponding depth dynamics, and the overall bioretention system water balance, respectively, as presented as follows:

$$\dot{L}(t) = \frac{1}{A_{TC}(\theta_{sat} - \theta_i)} (Q_{inf}(t) - Q_{out,u}(t) - Q_{exf}(t)) \quad (S6a)$$

$$\dot{h}_p(t) = \frac{1}{A_{TC}} (Q_{in}(t) - Q_{out,w}(t) - Q_{inf}(t)) \quad (S6b)$$

$$\dot{S}(t) = Q_{in}(t) - Q_{out}(t) - Q_{exf}(t) \quad (S6c)$$

1) Bioretention Flow Algebraic Constraints

The proposed model routes an inflow hydrograph through a bioretention system using physically-based stage-discharge relationships for the underdrain and weir flow. The underdrain and the weir are modeled using standard orifice and weir equations Eqs. (S7b) and (S7c). The underdrain flow is constrained to the infiltration rate and by the hydraulic capacity of the underdrain. Equations for several types of weirs are available in the model, including rectangular and triangular weirs. In this paper, we present the derivation for the triangular weir only. The lateral and bottom exfiltration are estimated using Eq. (S7d). The bottom exfiltration is only assumed in cases where the wetting front reached the bioretention bottom. Exfiltration process through the walls and bottom are estimated according to [7] based on Darcy's law, neglecting the exfiltration suction head. The average lateral exfiltration is a function of a triangular hydraulic gradient depending on the ponding depth and internal water storage, whereas the bottom exfiltration has a constant hydraulic gradient depending on the hydraulic pressure of the wetting front. We can write all flow algebraic constraints as:

$$Q_{out}(t) = Q_{out,u}(t) + Q_{out,w}(t) + Q_{exf}(t) \quad (S7a)$$

$$Q_{out,u}(t) = \begin{cases} \text{If } L(1 : t) \geq L_d \\ \min \left(n_1 A_o C_{d,u} \sqrt{2g(L(t) + h(t) - IWS)}, q_{per}(t) A_{TC} \right), \\ \text{Else} \\ 0 \end{cases} \quad (S7b)$$

$$Q_{out,w}(t) = 1.4n_2 \max \left[(h(t) - p)^{3/2}, 0 \right] \quad (S7c)$$

$$Q_{\text{exf}}(t) = \begin{cases} \text{If } L(1:t) \geq L_d \\ \frac{Q_{\text{exf},l}(t)}{K_{\text{sat},l} 2s(\frac{h(t)+L(t)/2}{L(t)/2})} + \frac{Q_{\text{exf},b}(t)}{K_{\text{sat},b} A_{\text{TC}} (\frac{h(t)+L(t)}{L(t)})} \\ \text{Else} \\ Q_{\text{exf},l}(t) \end{cases} \quad (\text{S7d})$$

$$Q_{\text{inf}}(t) = \frac{\min(C(t), P(t)) A_{\text{TC}}}{3.6 \times 10^6} \quad (\text{S7e})$$

Moreover, we collect a non-linear vector of flows such that $\Phi_2(t) = [Q_{\text{out}}(t), Q_{\text{out},u}(t), Q_{\text{out},w}(t), Q_{\text{exf}}(t), Q_{\text{inf}}(t), Q_{\text{per}}(t)]^T$ and apply it in Eq. (S1), resulting in a DAE state-space model given by:

$$\underbrace{\begin{bmatrix} \mathbf{I}_3 & \mathbf{0}_{3 \times 6} \\ \mathbf{0}_{6 \times 3} & \mathbf{O}_6 \end{bmatrix}}_E \underbrace{\begin{bmatrix} \dot{L}(t) \\ \dot{h}_p(t) \\ \dot{S}(t) \\ \dot{x}_2(t) \end{bmatrix}}_{\dot{\mathbf{x}}(t)} = \underbrace{\begin{bmatrix} \mathbf{I}_3 & \mathbf{0}_{3 \times 6} \\ \mathbf{0}_{6 \times 3} & -\mathbf{I}_6 \end{bmatrix}}_A \underbrace{\begin{bmatrix} \mathbf{x}_1(t) \\ \mathbf{x}_2(t) \end{bmatrix}}_{\mathbf{x}(t)} + \underbrace{\begin{bmatrix} \frac{1}{A_{\text{TC}}(\theta_{\text{sat}} - \theta_i)} (Q_{\text{per}}(t) - Q_{\text{out},u}(t) - Q_{\text{exf}}(t)) \\ \frac{1}{A_{\text{TC}}} (Q_{\text{in}}(t) - Q_{\text{out},w}(t) - s_{\text{inf}} Q_{\text{inf}}(t)) \\ Q_{\text{in}}(t) - Q_{\text{out}}(t) - Q_{\text{exf}}(t) \\ \Phi_2(t) \end{bmatrix}}_{\Phi(\mathbf{x}(t))} \quad (\text{S8})$$

where $s_{\text{inf}} = 1$ if $q_{\text{in}} > 0$, otherwise $s_{\text{inf}} = 0$.

Another boundary condition is applied in Eq. (S8). First, if $L(t + \Delta t) > L_d$, the stored depth would be larger than the bioretention maximum storage depth. Let $\gamma = L(t + \Delta t) - L(t)$; therefore, the ponding zone layer would receive a volume of $\gamma A_{\text{TC}}(\theta_{\text{sat}} - \theta_i)$. In this case, we impose $L(t + \Delta t) =$

L_d and increase the ponding zone water balance differential equation by the rate $\gamma(\theta_{\text{sat}} - \theta_i)$.

To solve Eq. (S8), we use a semi-implicit numerical scheme in the water balance dynamics. Assuming a finite-difference time Δt , we can write the following expression expanding Eq. (S6c) into:

$$\frac{S(t + \Delta t) - S(t)}{\Delta t} = \frac{1}{2} (Q_{\text{in}}(t + \Delta t) + Q_{\text{in}}(t) - Q_{\text{out}}(t + \Delta t) - Q_{\text{out}}(t) - Q_{\text{exf}}(t + \Delta t) - Q_{\text{exf}}(t)) \quad (\text{S9})$$

This method is named Level-Pool-Routing [8]–[10] and is applied to solve Eq. (S6c). We develop auxiliary tables that are built based on the flow governing equations for each flow condition [10]. To consider internal water storage, we can change the flow-discharge relationship from the auxiliary tables to allow flow only occurring when the internal water level is larger than the internal water storage. This method requires the calculation of the factor $\alpha(t)$ for each time-

step and require searches in the tables to solve the state variables for the next time-step. Alternatively, Eq. (S9) can be solved with numerical methods as Newton-Raphson [11]. From Eq. (S9), it is noted that all variables from time t are known and also $Q_{\text{in}}(t + \Delta t)$ is known since we assume an input net-rainfall data that can be converted into inflow from Eq. S3. Therefore, we can organize Eq. (S9) into known and unknown values as follows:

$$f(L(t + \Delta t), h(t + \Delta t), S(t + \Delta t)) = \underbrace{Q_{\text{in}}(t) + Q_{\text{in}}(t + \Delta t)}_{\text{Known Value}} + \underbrace{\left(\frac{2S(t)}{60\Delta t} - Q_{\text{out}}(t) \right)}_{\text{Known Value}} = \underbrace{\left(\frac{2S(t + \Delta t)}{60\Delta t} + Q_{\text{out}}(t + \Delta t) \right)}_{\text{Unknown Value}} \quad (\text{S10})$$

where f is a non-linear function relating inflows, outflows, and storage.

After computing the known value from Eq. (S10), we can find $\mathbf{x}_1(t + \Delta t)$ by solving $f^{-1}(\mathbf{x}_1(t + \Delta t))$. This process is performed using the Microsoft Excel ® searching functions. All the state variables (storage volume, ponding depth, saturation depth) are updated at each model time step and the process continues until the pre-defined routing time.

II. SOFTWARE TC-HYDRO

Here in this section, we detail the TC-Hydro version in Microsoft Excel. To run, the model is required a license version of Microsoft Excel 2013 or higher. Moreover, add-ins as the Solver and Developer modes should be activated for better performance of the software. Although most of the calculations are performed in spreadsheets, the integration within the data entry and the spreadsheet is fully done using guided user forms (GUI). After opening the file, the user must

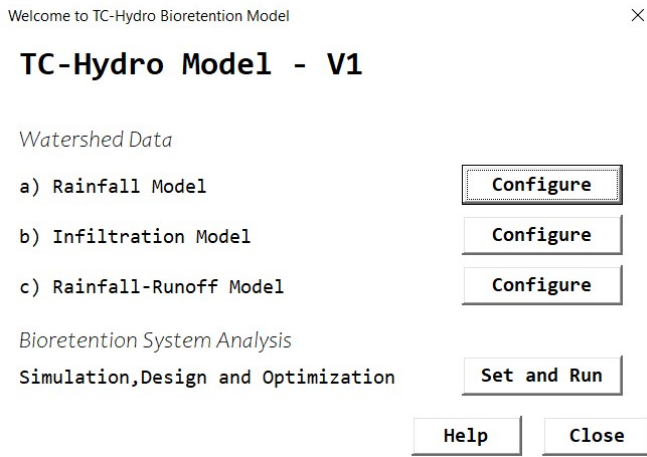


Fig. S1: Initial Interface of the TC-Hydro V1, where the models of rainfall, infiltration, rainfall-runoff, and simulation, design, and optimization.

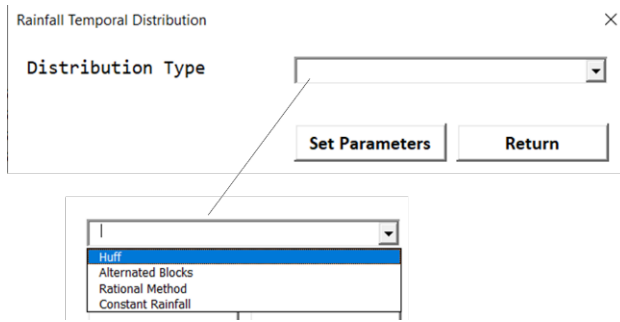


Fig. S2: Rainfall Temporal Distribution Models

$$P(t) = 0.2558\left(\frac{t}{t_d}\right)^4 + 1.5586\left(\frac{t}{t_d}\right)^3 - 4.346\left(\frac{t}{t_d}\right)^2 + 3.603\left(\frac{t}{t_d}\right) - 0.0579 \quad (\text{S12a})$$

$$P(t) = 6.1888\left(\frac{t}{t_d}\right)^4 - 14.996\left(\frac{t}{t_d}\right)^3 + 10.861\left(\frac{t}{t_d}\right)^2 - 1.0758\left(\frac{t}{t_d}\right) + 0.0235 \quad (\text{S12b})$$

$$P(t) = 71.986\left(\frac{t}{t_d}\right)^6 + 206.68\left(\frac{t}{t_d}\right)^5 - 211.78\left(\frac{t}{t_d}\right)^4 - 92.488\left(\frac{t}{t_d}\right)^3 + 16.973\left(\frac{t}{t_d}\right)^2 - 0.5697\left(\frac{t}{t_d}\right) + 0.0041 \quad (\text{S12c})$$

$$P(t) = -58.036\left(\frac{t}{t_d}\right)^6 + 154.96\left(\frac{t}{t_d}\right)^5 - 151.59\left(\frac{t}{t_d}\right)^4 + 68.269\left(\frac{t}{t_d}\right)^3 - 13.978\left(\frac{t}{t_d}\right)^2 + 1.3842\left(\frac{t}{t_d}\right) - 0.008 \quad (\text{S12d})$$

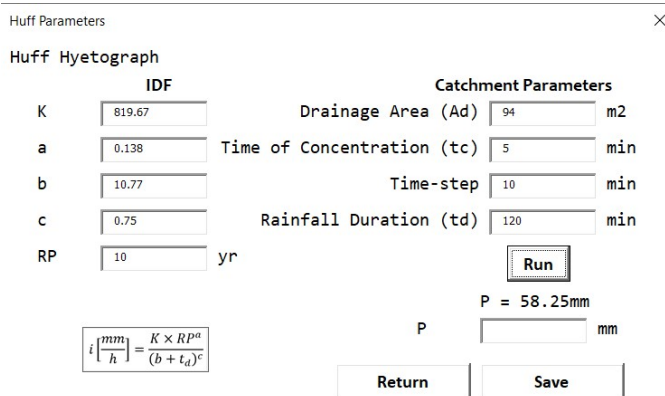


Fig. S3: Huff Hyetograph parameters. After clicking in Run, a calculated precipitation is shown, and the user needs to enter the assumed precipitation in the respective text box that could be exactly the one calculated or a different value.

habilitate the content and enable macros. The initial user form in the software is activated after enabling edition and macros. It guides the user to the watershed data entry and through the bioretention system analysis modules. The user must follow steps (a), (b), and (c) to start the bioretention system analysis as shown in Fig. S1.

A. Rainfall Temporal Distribution Models

Four temporal rainfall distribution models are available in the model, including Huff, Alternated Blocks, Rational Method and Constant Rainfall methods as presented in Fig. S2.

1) Huff Hyetograph

The Huff hyetographs are a set of polynomial equations and are developed for the 1st, 2nd, 3rd and 4th quartile, depending on the rainfall duration. Basically, it distributes the entered precipitation according to the respective quartile equation. It is required a Sherman Type IDF curve, such that

$$i = \frac{K \cdot RP^a}{(b + t_d)^c} \quad (\text{S11})$$

where i is the rainfall intensity in mm/h, K , a , b and c are fitted parameters for the IDF and RP is the return period of the rainfall.

The polynomial equations used in the software (Fig. S3) to represent the Huff temporal distribution are presented as follows:

where Eqs (S12a), (S12b), (S12c), and (S12d) represent polynomial equations for Huff's 1st, 2nd, 3rd, and 4th quartiles, respectively. Variables t and t_d are the time and the rainfall duration.

2) Alternated Blocks

The alternated blocks also require the IDF and the catchment parameters and has two main governing equations for rainfall intensity before and after the rainfall peak.

$$i(t) = \frac{KRP^a \left(\frac{t_1}{\gamma} (1 - c) + b \right)}{\left(\frac{t_1}{\gamma} + b \right)^{1+c}} \quad \text{for } t = t_1 \leq \gamma t_d \quad (\text{S13a})$$

$$i(t) = \frac{KRP^a \left(\frac{t_2}{\gamma} (1 - c) + b \right)}{\left(\frac{t_1}{1-\gamma} + b \right)^{1+c}} \quad \text{for } t = t_2 > \gamma t_d \quad (\text{S13b})$$

where γ is a peak factor assumed as 0.5 to represent the rainfall peak at 50% of the storm duration and Eqs. (S13a) and (S13b) represent equations for durations before peak and after peak.

Fig. S4: Alternated Blocks User Interface where the IDF and the Catchment parameters are entered

Fig. S5: Rational Method Parameters, where the IDF and the Catchment parameters are entered

Data entry for this section is shown in Fig. S4.

3) Rational Method

The rational method hyetograph assumes a constant rainfall with an intensity given by the IDF curve through the duration of the storm t_d , as shown in Fig. S5.

4) Constant Rainfall

The constant rainfall basically assumes a constant rainfall intensity entered the respective text box (see Fig. S6. In the case of the constant rainfall equals the calculated rainfall from the IDF, the method is hence equivalent to the Rational Method.

Fig. S6: Parameters for the Constant Rainfall Module where the IDF and the Catchment parameters are entered

B. Catchment Infiltration Model

For the infiltration, three models are available – the SCS-CN, the Horton Method, and the Rational Method (see Fig. S7). For the SCS method is required the curve-number (CN) of the catchment, and for the Horton method, the initial and final infiltration rates as well as the decreasing exponential factor k are required, whereas for the Rational Method, only the runoff coefficient is necessary. The Rational Method, however, is only possible to be selected in case the Rational Method was chosen for the temporal distribution method.

1) SCS Method

The standard equations for the SCS-CN method are solved to estimate the effective precipitation and infiltration rates (see Fig. S8). The effective precipitation, accumulated rainfall, catchment storage capacity, accumulated infiltration, infiltration rate, and incremental effective precipitation are presented below, respectively.

$$S = \frac{25400}{CN} \quad (S14a)$$

$$P_{ef}(t) = \frac{P(t) - 0.2S}{2P(t) + 0.8S} \geq 0.2S \quad (S14b)$$

$$P(t) = \sum_{k=1}^t i(k) \Delta t \quad (S14c)$$

$$F(t) = P(t) - P_{ef}(t) \quad (S14d)$$

$$f(t + \Delta t) = \frac{F(t + \Delta t) - F(t)}{\Delta t} \quad (S14e)$$

$$\Delta P_{ef}(t + \Delta t) = P_{ef}(t + \Delta t) - P_{ef}(t) \quad (S14f)$$

where P_{ef} is the accumulated effective precipitation in mm, P is the accumulated rainfall, k is a time-step index, S is the storage capacity in mm, $F(t)$ is the accumulated infiltration, $f(t)$ is the infiltration rate, and ΔP_{ef} is the incremental precipitation.

2) Horton Method

The infiltration capacity equation is given by an exponential equation that requires three parameters, f_c (final infiltration in mm/h), f_0 (initial infiltration in mm/h) and k (decreasing exponential factor in 1/h) (see Fig. S9). The infiltration rate, accumulated infiltration, effective precipitation rate, accumulated precipitation and incremental precipitation are presented below, respectively.

$$f(t) = f_c + (f_0 - f_c) \exp^{-kt} \quad (S15a)$$

$$F(t) = \sum_{k=1}^t f(k) \Delta t \quad (S15b)$$

$$p_{ef}(t + \Delta t) = i(t + \Delta t) - \frac{f(t + \Delta t) - f(t)}{2} \quad (S15c)$$

$$P_{ef}(t) = \sum_{i=1}^t p_{ef}(i) \Delta t \quad (S15d)$$

$$\Delta P_{ef}(t) = p_{ef}(t) \Delta t \quad (S15e)$$

where $i(t)$ is the rainfall intensity and $p_{ef}(t)$ is the effective precipitation rate in mm/h.

Fig. S7: Infiltration models selection, where two possibilities are shown: SCS method and Horton Method

Fig. S8: SCS-CN user form where the Curve-Number.

3) Rational Method

To simulate the infiltration model with the Rational Method, only an entry of the runoff coefficient is necessary, as shown in Fig. S10.

C. Rainfall Runoff Model

For the conversion of excess of precipitation into flow discharge, three models are available – the Santa Barbara Urban Hydrograph (SBUH), the SCS PRF 484 unit hydrograph and the Rational Method Hydrograph (see Fig. S11).

For all methods is required to set the simulation time in minutes.

1) Santa Barbara Unit Hydrograph (SBUH)

Assuming a linear reservoir with a damping constant K_r proportional to the time of concentration of the catchment, the hydrograph of the SBUH method is developed assuming the flow discharge linearly proportional to the runoff volume, as a linear reservoir (see Fig. S12). The governing equations of this method are presented below.

$$I(t) = (i(t)d + i_e(1 - d))A \quad (S16a)$$

$$K_r = \frac{\Delta t}{2t_c + \Delta t} \quad (S16b)$$

Fig. S9: Horton Parameters, where parameters f_c , and k can be estimated in databases as the ones provided in HEC-HMS manuals or field estimated with infiltration tests

Fig. S10: Rational Method, Runoff Coefficient.

Fig. S11: Rainfall-Runoff model selection, where two alternatives are possible: the SBUH and the SCS methods

$$Q_{\text{runon}}(t + \Delta t) = Q_{\text{runon}}(t) + K_r \left(I(t) + I(t + \Delta t) - 2Q_{\text{runon}}(t) \right) \quad (S16c)$$

where I is the effective precipitation for pervious and impervious areas, d is the percentage of impervious areas directly connected to the catchment, i_e is the effective precipitation for the pervious areas, K_r is the reservoir damping parameter and Q is the flow discharge in the outlet of the catchment.

2) SCS Unit Hydrograph Method

The software allows the convolution of 432 unit hydrographs, which is equivalent to a daily rainfall with 5-min time-steps in an impermeable watershed (i.e., $C = 1$, $d = 1$, $CN = 100$, $f_0 = f_c = 0$). The following equations present the parameters required for the unit hydrograph and for the convolution of all blocks of effective precipitation.

$$t_L = 0.6t_c \quad (S17a)$$

$$t_p = \frac{\Delta t}{2} + t_L \quad (S17b)$$

$$t_b = 2.67t_p \quad (S17c)$$

$$q_p = 2.05 \frac{A_d}{t_p} \quad (S17d)$$

$$p_{\text{ef}}(t) = \frac{dP_{\text{ef}}(t)}{dt} \quad (S17e)$$

Fig. S12: Parameters of the SBUH, where d is the percentage of impervious directly connected areas

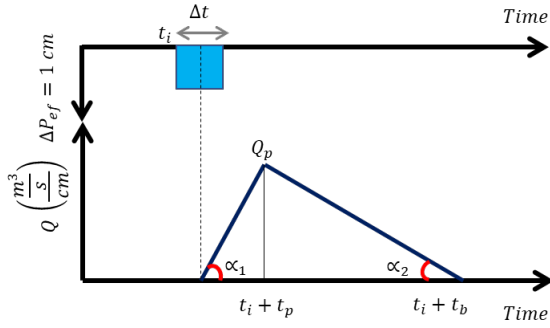


Fig. S13: Scheme of the unit hydrograph.

$$\begin{aligned}
 Q_{\text{runon}}(t) &= p_{\text{ef}} * q(t) \\
 &= \int_0^t p_{\text{ef}}(\tau) q(t - \tau) d\tau \\
 &= \sum_{i=1}^t \Delta P_{\text{ef}}(i) U_{i-1+1} \quad (S17f)
 \end{aligned}$$

where Δt is the simulation time in minutes, τ is a convolution parameter, U is the ordinate of the unit hydrograph and can be calculated defining two slopes, α_1 and α_2 , such that:

$$\tan \alpha_1 = \frac{q_p}{t_p} \quad (S18a)$$

$$\tan \alpha_2 = -\frac{q_p}{t_b - t_p} \quad (S18b)$$

These angles are also shown in Fig. S13.

Therefore, using geometry relationships, we can determine two functions for the ordinates of the unit hydrograph and hence solve the convolution integral in a time-step fashion. Assuming a block of effective precipitation with a timespan of t_i from the beginning of the event, the flow conversion for this block depends on the actual model time, such that:

$$Q_n(t) = 0, \text{ If } t \leq t_i \quad (S19a)$$

$$Q_n(t) = (t - t_i) \tan \alpha_1 \text{ If } t_i \leq t \leq t_i + t_p \quad (S19b)$$

$$Q_n(t) = (t - t_p) \tan \alpha_2 \text{ If } t_i + t_p \leq t \leq t_i + t_b \quad (S19c)$$

$$Q_n(t) = 0, \text{ Otherwise} \quad (S19d)$$

Therefore, the total flow observed in a time t can be expressed as:

$$Q_{\text{runon}}(t) = \sum_{n=1}^k Q_n(t) \quad (S20)$$

where k is the number of blocks of effective precipitation and n represents the order of the blocks of effective precipitation.

3) Rational Method

The rational method hydrograph be either a trapezoid or an isosceles triangle, depending on the rainfall duration and time of concentration of the catchment. Essentially, three cases are possible:

a) Case where $t_d \leq t_c$

$$Q_{\text{runon}}(t) = CiA \left(1 - \frac{t_c - t}{t_c}\right) \text{ If } t \leq t_c \quad (S21a)$$

$$Q_{\text{runon}}(t) = CiA \left(1 - \frac{t - t_d}{t_c}\right) \text{ If } t_c < t \leq t_c + t_d \quad (S21b)$$

$$Q_{\text{runon}}(t) = 0 \text{ Otherwise} \quad (S21c)$$

b) Case where $t_d \leq t_c$

$$Q_{\text{runon}}(t) = CiA \left(1 - \frac{t_c - t}{t_c}\right) \text{ If } t \leq t_c \quad (S22a)$$

$$Q_{\text{runon}}(t) = CiA \text{ If } t_c \leq t \leq t_d \quad (S22b)$$

$$Q_{\text{runon}}(t) = CiA \left(1 - \frac{t - t_d}{t_c}\right) \text{ If } t_d \leq t \leq t_d + t_c \quad (S22c)$$

$$Q_{\text{runon}}(t) = 0 \quad (S22d)$$

where C is the runoff coefficient and t_c is the time of concentration of the catchment.

In cases where the rainfall duration is larger than $2t_c$, a trapezoidal hydrograph is developed assuming the constant inflow peak through a duration $(t_d - t_c)$ from t_c .

D. Bioretention System Analysis

After the configuration of the catchment models, a main userform is shown (see Fig. S14) presenting the dimensions and parameters required to simulate the bioretention system.

1) Weir Parameters

For the weir configuration, two options are allowed (see Fig. S15). The triangular weir, also called as Thompson or V-notch weir and the Francis weir or rectangular weir with a lateral contraction.

2) Run simulation and Save Parameters

The simulation results are showed according to the data entered in the main interface (see Fig. S16).

3) One-at-the-time Sensitivity Analysis

The one-at-the-time sensitivity analysis is performed considering the base scenario provided by the entered data in the main userform (see Fig. S17). Moreover, it is required to enter the beginning (e.g., 0%), the interval (e.g., 90% positive and negative variation) and the steps. The exfiltration parameters must be entered in this userform even with the bioretention is lined, in order to assess the role of exfiltration in the modeled system. Results of the simulation are shown in Fig. S18.

4) Critical Rainfall Duration

The critical duration is calculated and presented in a graph, as showed in Fig. S19.

5) Box-Plot Hydrograph

A statistical box-plot hydrograph is developed assuming 486 modeling results varying the rainfall temporal distribution, infiltration properties and initial storage in terms of minimum and maximum values from Fig. S20. Possible results of this simulation are shown in Fig. S21.

6) Optimization Module

A single objective optimization problem is designed assuming a cost function given by the volume, area, ponding depth and a penalizing function in terms of a required minimum peak flow mitigation (see Fig. S22). Weights are given to represent the desire of the designer in the optimization.

Let $\mathbf{x}_d = [L, B, L_d, p, k_{\text{sat}}, \theta_{\text{sat}}, \psi]^T$ representing the geometrical and soil media decision variables one should do to design a bioretention system. Moreover, given a cost function representing the volume, surface area, ponding depth volume, and peak flow reduction, one can write:

$$\text{Cost} = \underbrace{k_1(LBL_d)}_{\text{Volume}} + \underbrace{k_2(LB)}_{\text{Area}} + \underbrace{k_3(LBp)}_{\text{Ponding depth}} + \underbrace{k_4(2sL_d)}_{\text{Perimeter}} + \underbrace{k_5 \max(\mathcal{P}_{\min} - \mathcal{P}, 0)}_{\text{PeakFlowReduction}} + \underbrace{k_6 \max(\max(h) - p, 0)}_{\text{Maximum Ponding Depth}} \quad (S23a)$$

Bioretention geometry, outflow devices and infiltration parameters

X

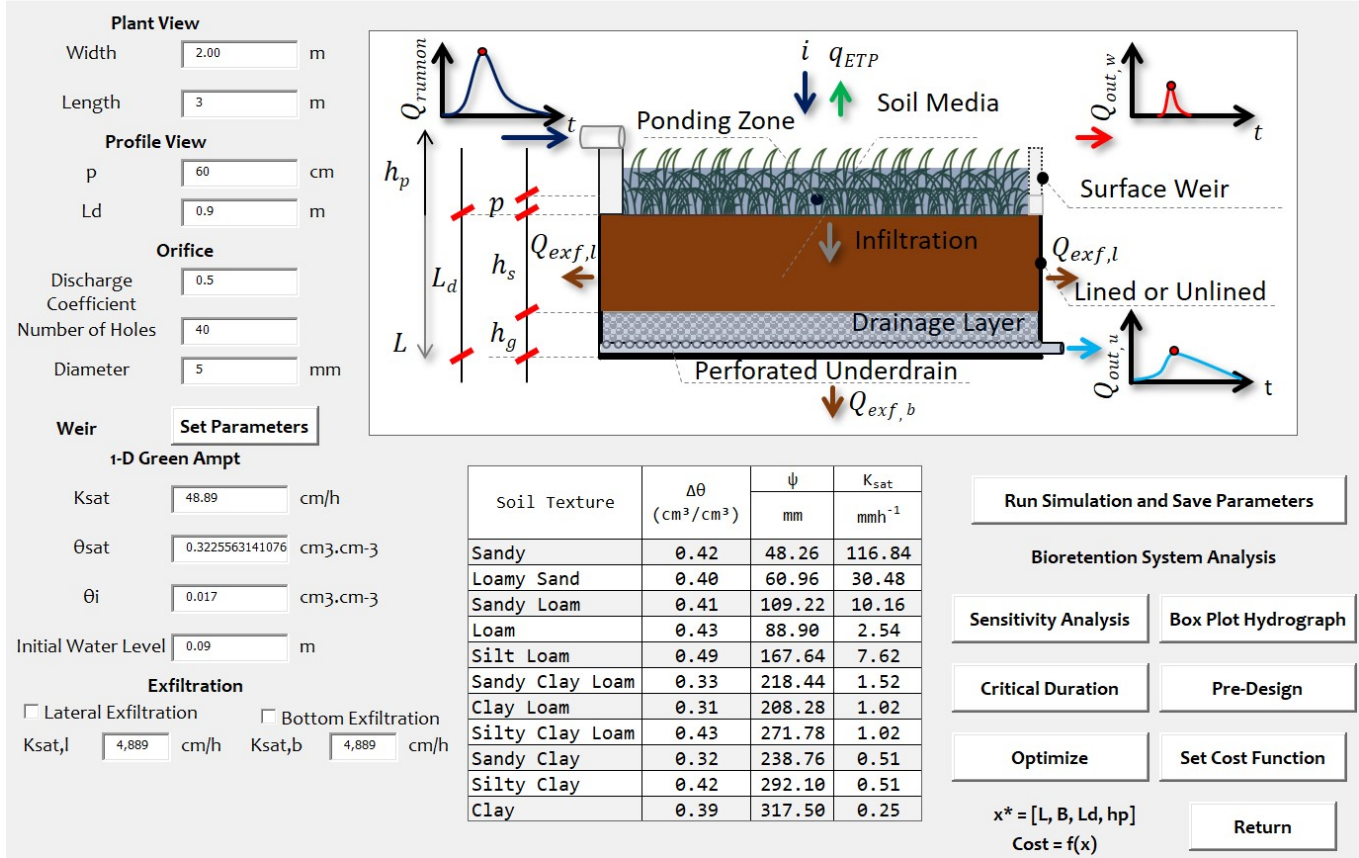


Fig. S14: Main Interface of the TC-Hydro showing the Plant View, Orifice, Weir, GA-1D, Exfiltration and Modeling Options.

$$P = \frac{\max(Q_{in}) - \max(Q_{out})}{\max Q_{in}} \quad (S23b)$$

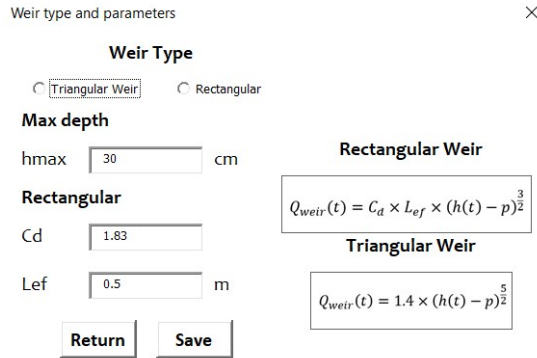


Fig. S15: Weir equations, types, and parameters

Therefore, the optimization problem is defined as:

$$\begin{aligned} \min_{x_d} \quad & \text{Eq. (S23a)} \\ \text{s.t.} \quad & \text{Eq. (S8)} \\ & x_{\min} \leq x_d \leq x_{\max} \end{aligned} \quad (S24)$$

After the configuration of the optimization problem, a genetic algorithm optimization problem with 100 population,

40 generations, mutation rate of 0.075 and computational time limited for 240 seconds is defined. The near optimal results are displayed in the interface, as showed in this Fig. S23.

7) Pre-Design Methods

The pre-design methods of the Water Quality Volume and Pre-development Flow Conditions are calculated assuming the following parameters.

The following equations represent the main calculations for the water quality volume and pre-development flow conditions volume.

i) Water Quality Volume

$$R_v = 0.05 + 0.9I_p \quad (S25)$$

ii) Pre-development Flow Conditions

$$\Delta P_{ef}^{PFC} = (P_{ef}^{post}(P^{post}, CN^{post}) - P_{ef}^{pre}(P^{pre}, CN^{pre})) \quad (S26a)$$

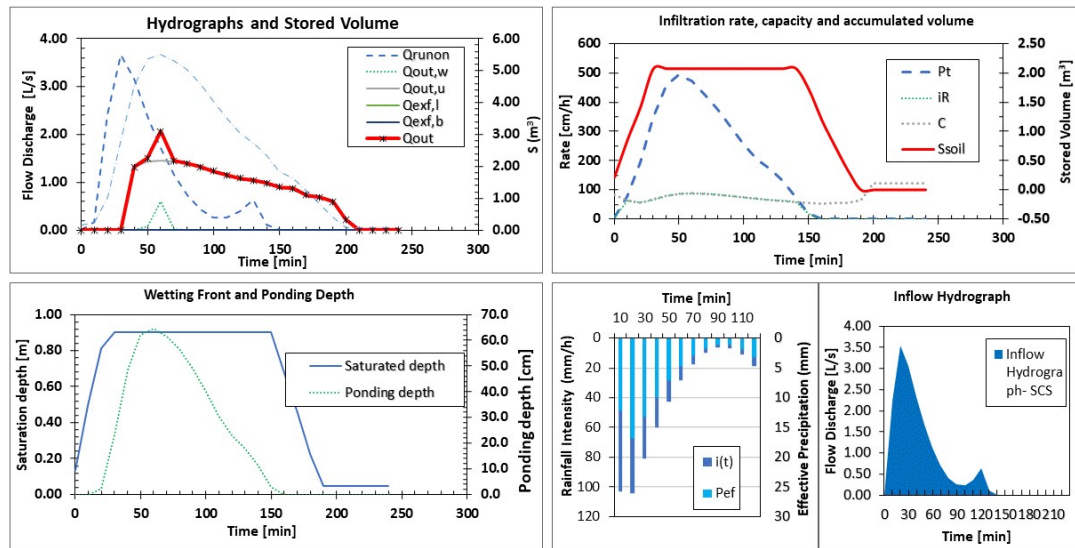
$$P^{post} = P^{post} = \max(P(2, 24), P(90\%)) \quad (S26b)$$

$$A^{WQV} = \frac{WQV}{L_d \eta} \quad (S26c)$$

$$A^{PFC} = \frac{A_d \Delta P_{ef}^{PFC}}{L_d \eta} \quad (S26d)$$

Simulation Results

X



Summary

| | | | | | |
|---------------------|---------|----------------|--------|----------------|---------|
| Max Outflow Peak | 2.06L/s | Residence Time | 3.00h | Inflow Volume | 10.4m³ |
| Peak Flow Reduction | 44% | Time to Peak | 60min | Orifice Volume | 10.71m³ |
| Max ponding depth | 64.5 | Max Storage | 5.52m³ | Weir Volume | 0.42m³ |

Return

Fig. S16: Results of the simulation where graphs show hydrographs, saturation depths, ponding depths, hyetographs, inflow hydrographs, and infiltration rates.

One-at-time Sensitivity Analysis

Parameters

Begin

Interval

Step

Ksat,l

Ksat,b

Return

Run

Fig. S17: Sensitivity Analysis Parameters, where the interval is the decimal percentage of variation and step is how the change in parameters are performed.

Sensitivity Analysis Results

X

Local Sensitivity Analysis

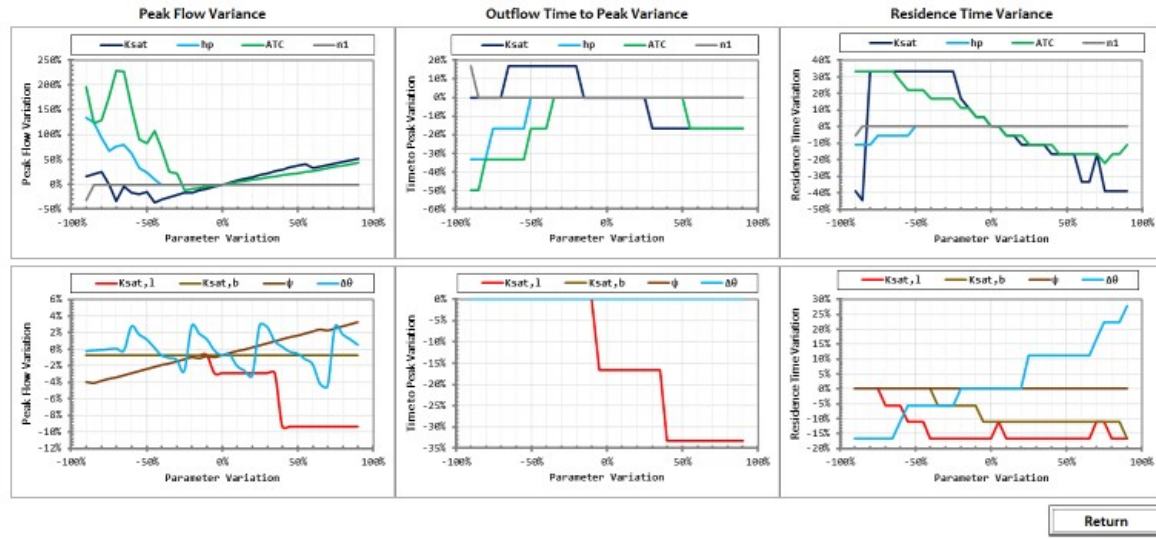


Fig. S18: Sensitivity Analysis Results where graphs are organized into most sensitive parameters (green, light blue, dark blue, grey)

Critical Duration Analysis

X

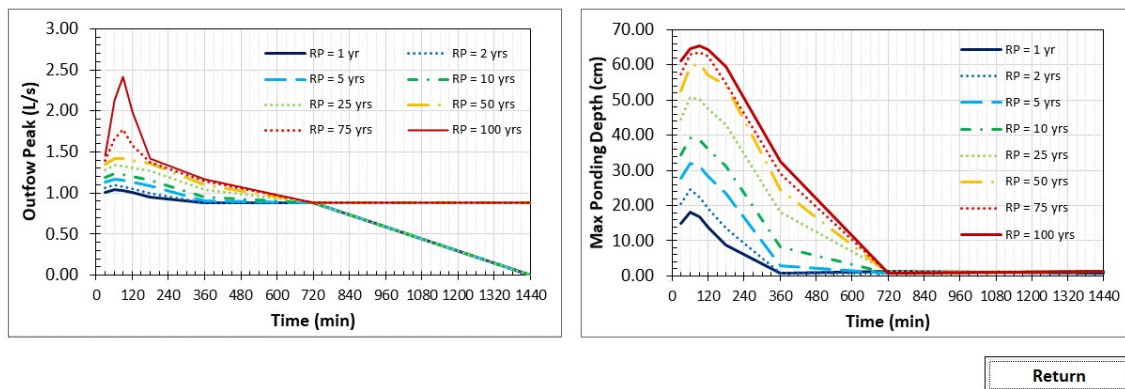


Fig. S19: - Critical Duration Analysis Result, where left chart shows outflow peaks, whereas right chart shows ponding depth

Box plot Hydrograph

X

Parameters

Saturation

min 0.1

max 1

Uncertainty

Rate 0.2

Return

Run

Fig. S20: Box-plot parameters, where min and max are the assessed saturation conditions and rate the variation in the estimated values

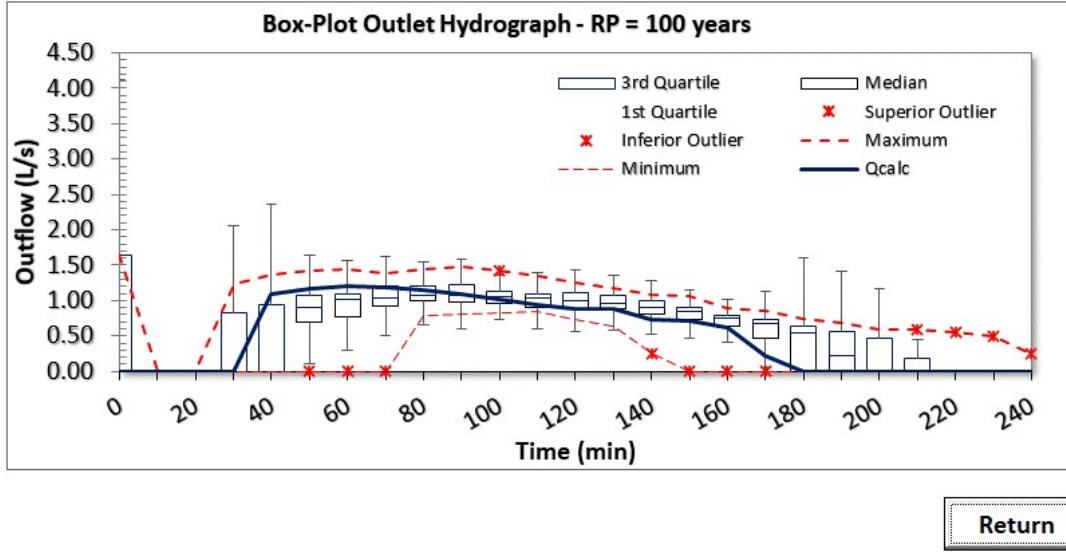


Fig. S21: Box-plot Graph showing statistical variation within modeled results from different scenarios

Optimization Constraints and Weights

| Min Values | | Max Values | |
|------------|-------|------------|-------|
| Lmin | 0.5 m | Lmin | 3 m |
| Bmin | 0.5 m | Bmin | 3 m |
| Ldmin | 0.3 m | Ldmin | 0.9 m |
| hpmin | 0 m | hpmin | 0.6 m |
| dQmin | 0.2 | | |

Return Save

$$Cost = f(L, B, L_d, h_p) = \overbrace{k_1 \times (L \times B \times L_d)}^{Volume} + \overbrace{k_2 \times (L \times B)}^{Area} + \overbrace{k_3 \times (L \times B \times h_p)}^{Ponding Depth} + \overbrace{k_4 \times [\max(dQ_{min} - dQ, 0)]}^{Peak Flow Reduction}$$

$$dQ = \frac{\max(Q_{in}) - Q_{out}^p}{\max(Q_{in})}$$

k1: 1 k2: 1 k3: 1 k4: 1000000

Fig. S22: Optimization Module Parameters

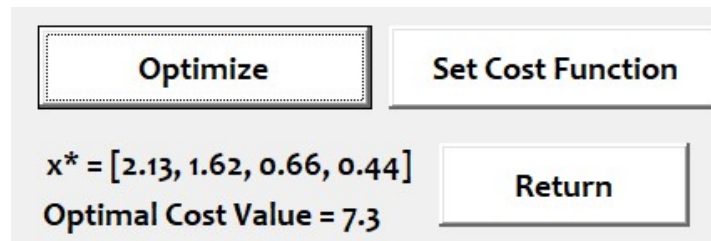


Fig. S23: Near-optimal results including decision variables and cost function evaluation

(S26e) pre-development flow conditions methods.

Data entry of these methods are shown in Fig. S24.

iii) Envelope Curve

$$\Delta h^{EC} = \arg \max \left(\int_0^{t_f} \left(i(t) - \frac{Q_{pre}}{A_d} \right) dt \right) \quad (S27a)$$

$$A^{EC} = \frac{A_d \Delta h^{EC}}{L_d \eta} \quad (S27b)$$

where R_v is the impervious connected area rate, $P(90\%)$ is the daily rainfall with 10% of exceedance of probability, P_{post} and P_{pre} are accumulated precipitations calculated based on the 2-yr, 24-h storm and $P(90\%)$, P_{ef}^{post} and P_{ef}^{pre} are effective precipitation of post and pre-development, η is the average porosity of the bioretention and A^{WQV} and A^{PFC} are the bioretention surface areas for the water quality volume and

III. IDF CURVE OF SÃO CARLOS

The IDF curve assumed to estimate the hydrographs is given by:

$$i(t_d) = \frac{819.67RP^{0.138}}{(10.77 + t_d)^{0.75}} \quad (S28)$$

IV. EVALUATION FUNCTIONS

For each perturbation in the assessed variables, a variance is calculated in terms of the baseline scenario results.

Pre-design Methods Parameters

✕

Pre-Design Methods**Assumed Parameters**Porosity Media Depth **Pre-development Flow Conditions**CNpre CNpost **Water Quality Volume****Enter Daily Rainfall**Imp. Rate **IDF**K a b c Return Period yr**Results****Return****Run****Fig. S24:** Pre-design parameters

a) Outflow Peak Variance (OPV)

$$OPV = \frac{\Delta Q^p}{Q_b^p}$$

(S29)

b) Time to Peak Variance (TPV)

$$TPV = \frac{\Delta t^p}{t_b^p}$$

(S30)

c) Residence Time Variance (RTV)

$$RTV = \frac{\Delta R^t}{R_b^t}$$

(S31)

where Q_{in} , Q_p , Q_b , t_p , and B are the inflow discharge, peak discharge, baseflow discharge, time to peak, and shape factor, respectively.

Values used in this analysis are $Q_p = 0.06 \text{ m}^3/\text{s}$, $Q_b = 0$, and $\beta = 2$.

B. Francis Weir

Parameters

$$Q_w(t) = c_1^w L_{ef}^w (\max(h - p, 0))^{c_2^w} \quad (S33)$$

where $c_1 = 1.8$, $L_{ef} = 1 \text{ m}$, and $c_2^w = 3/2$.

V. SWMM COMPARISON*A. Inflow Hydrograph*

The inflow hydrograph is simulated with a Nash function, given by:

$$Q_{in}(t) = (Q_p - Q_b) \left(\frac{t}{t_p} \exp \left\{ 1 - \frac{t}{t_p} \right\} \right)^\beta \quad (S32)$$

VI. RESULTS OF OPTIMIZATION MODELING

The modeling results of the near-optimal design for the bioretention in Numerical Case Study 3 are shown in Fig. S25.

REFERENCES

- [1] M. B. d. Macedo, C. A. F. d. Lago, E. M. Mendiando, and V. C. B. d. Souza, "Performance of bioretention experimental devices: contrasting

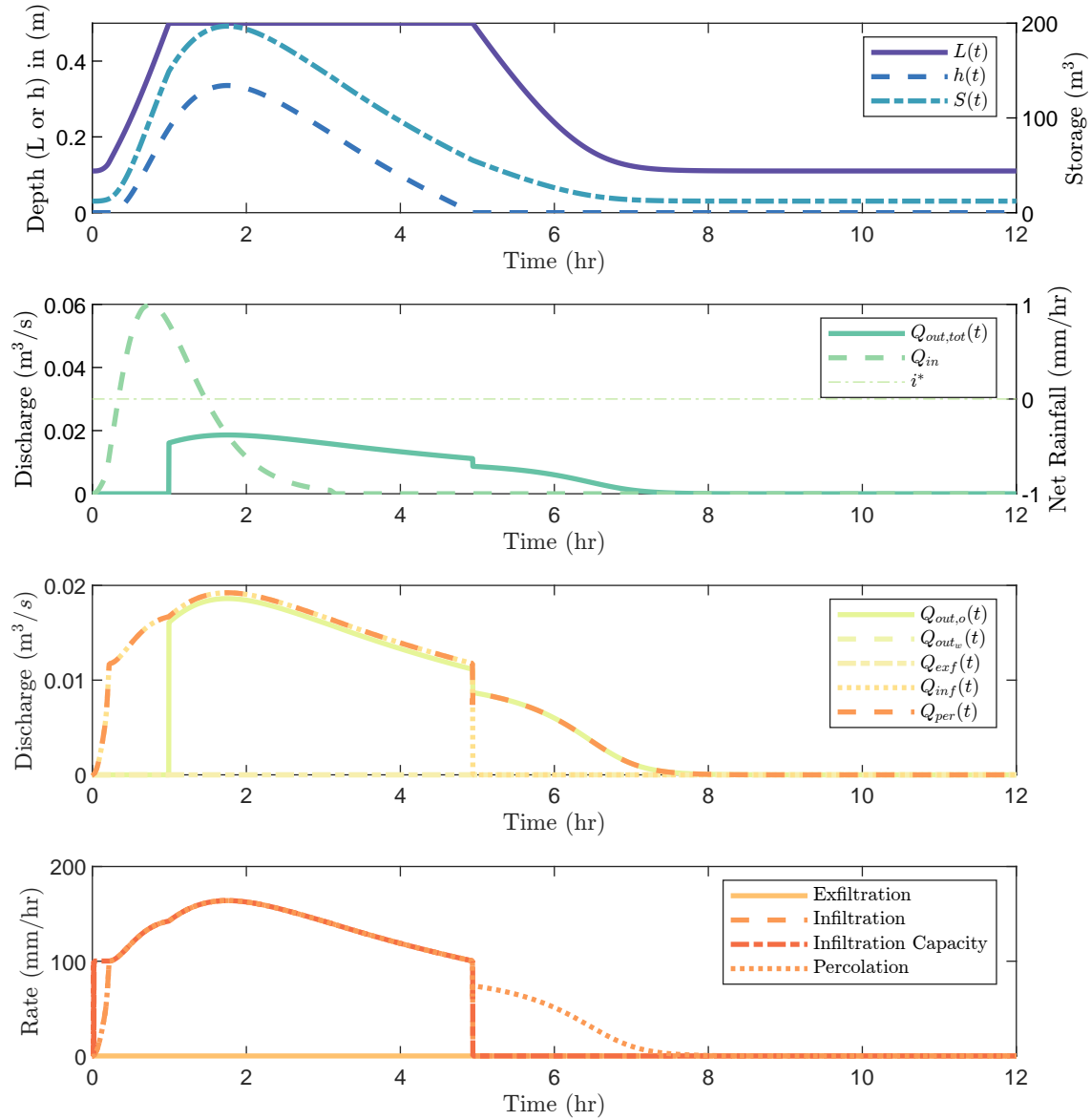


Fig. S25: Simulation results for the most cost-effective solution from the optimization problem solutions.

| Solution | Pop. | Gen. | A_{TC} (m^2) | L_d (m) | k_{sat} (cm/hr) | p(m) | Computational time (sec) | Cost (USD) |
|----------|------|------|--------------------|-----------|-------------------|------|--------------------------|------------|
| 1 | 40 | 40 | 596.09 | 0.51 | 4.49 | 0.39 | 804 | 42,246 |
| 2 | 40 | 20 | 382.94 | 0.72 | 6.41 | 0.29 | 496 | 30,526 |
| 3 | 40 | 10 | 422.02 | 0.50 | 9.50 | 0.39 | 231 | 29,826 |
| 4 | 20 | 40 | 645.79 | 0.51 | 9.35 | 0.27 | 420 | 45,631 |
| 5 | 20 | 20 | 564.74 | 0.55 | 8.11 | 0.38 | 154 | 40,990 |
| 6 | 20 | 10 | 563.68 | 0.56 | 8.10 | 0.26 | 73 | 41,172 |
| 7 | 10 | 40 | 634.86 | 0.50 | 6.22 | 0.23 | 57 | 44,692 |
| 8 | 10 | 20 | 503.52 | 0.85 | 6.77 | 0.34 | 69 | 42,749 |
| 9 | 10 | 10 | 669.45 | 0.51 | 6.18 | 0.40 | 39 | 47,431 |

TABLE S2: Near-optimal results for different size of population and generation using the single objective Genetic Algorithm.

- laboratory and field scales through controlled experiments,” *RBRH*, vol. 23, 2018.
- [2] Z. He and A. P. Davis, “Process modeling of storm-water flow in a bioretention cell,” *Journal of Irrigation and Drainage Engineering*, vol. 137, no. 3, pp. 121–131, 2011.
 - [3] A. O. Akan, “Preliminary design aid for bioretention filters,” *Journal of Hydrologic Engineering*, vol. 18, no. 3, pp. 318–323, 2013.
 - [4] W. H. Green and G. Ampt, “Studies on soil physics,” *The Journal of Agricultural Science*, vol. 4, no. 1, pp. 1–24, 1911.
 - [5] S. Gülbaz and C. M. Kazezyılmaz-Alhan, “Hydrological model of lid with rainfall-watershed-bioretention system,” *Water Resources Management*, vol. 31, no. 6, pp. 1931–1946, 2017.
 - [6] A. J. Chorin, J. E. Marsden, and J. E. Marsden, *A mathematical introduction to fluid mechanics*. Springer, 1990, vol. 168.
 - [7] J. G. Lee, M. Borst, R. A. Brown, L. Rossman, and M. A. Simon, “Modeling the hydrologic processes of a permeable pavement system,” *Journal of Hydrologic Engineering*, vol. 20, no. 5, p. 04014070, 2015.
 - [8] L. T. L. M. Ferreira, M. G. F. P. d. Neves, and V. C. B. d. Souza, “Puls method for events simulation in a lot scale bioretention device,” *RBRH*, vol. 24, 2019.
 - [9] R. A. Wurbs, *Modeling and analysis of reservoir system operations*. Prentice Hall, 1996.
 - [10] M. N. Gomes Jr, E. M. Mendiando, F. Dornelles, A. T. Papagiannakis, and M. H. Giacomoni, “Permeable pavement hydrological model to assess the long-term efficiency of maintenance using high-resolution temperature and rainfall data,” in *World Environmental and Water Resources Congress 2021*, 2021, pp. 1103–1117.
 - [11] T. J. Ypma, “Historical development of the newton–raphson method,” *SIAM review*, vol. 37, no. 4, pp. 531–551, 1995.